Dynamics of self-assembled surfactant systems

Cite as: J. Chem. Phys. **108**, 2232 (1998); https://doi.org/10.1063/1.475604
Submitted: 24 June 1997 . Accepted: 20 October 1997 . Published Online: 04 June 1998

Friedrich K. von Gottberg, Kenneth A. Smith, and T. Alan Hatton

Dynamics of self-assembled surfactant systems

Friedrich K. von Gottberg, Kenneth A. Smith, and T. Alan Hatton
Department of Chemical Engineering, Massachusetts Institute of Technology, Cambridge, Massachusetts 02139

(Received 24 June 1997; accepted 20 October 1997)

The dynamics of self-assembling systems were investigated for the model amphiphile A_2B_2 using stochastic dynamic simulations. Temperature jump computer ''experiments'' were performed and the evolution of the system to its new equilibrium state monitored. The results were interpreted based on the Aniansson–Wall theory of micellar kinetics. The transient behavior predicted using the Aniansson–Wall theory agrees well with the simulated data, particularly at short times. At long times, deviations are observed which may be ascribed to errors in estimating the dissociation rate and number density of aggregates in the all important micelle-depleted zone. The micellar dissociation constant was calculated from independent tagging simulations. The amphiphile exit rate constant was calculated at different temperatures from which an activation energy associated with the removal of a surfactant chain from a micelle was found to be of order 10–15 kT and to be independent of the friction coefficient. Finally the Helmholtz free energy profile associated with the extraction of a surfactant chain from a micelle was determined. A free energy barrier height of order 5 kT was obtained. Kramers' rate theory was employed to determine the corresponding exit rate constant which was found to be in excellent agreement with the results obtained from tagging runs. The barrier height associated with the insertion of a surfactant chain was order 1 kT, suggesting that the association process is diffusion controlled. [S0021-9606(98)50105-5]

I. INTRODUCTION

In a previous paper[1] we demonstrated the ability to determine the equilibrium properties of a model amphiphile system of type A_2B_2 (A=hydrophilic, B=hydrophobic) using stochastic dynamics simulations. In this paper we wish to look at the dynamic processes involved in such micellar systems, in particular the exit and entry rates of surfactants into micelles and the response of the system to a temperature perturbation.

Temperature, pressure, and concentration jump experiments have long been employed by experimentalists to elucidate dynamic phenomena in micelle solutions.[2] A perturbation is introduced, and the response of the system is monitored, typically using light scattering or absorbance. The general consensus is that there are two relaxation processes—a fast step associated with the exchange of surfactants between the bulk and micellar phases (nano-microsecond time range), and a second slower process associated with the breakup (dissolution) or formation of new micelles (micro-milliseconds).[3] In ionic systems, an extremely fast process is sometimes observed and is ascribed to the rearrangement of counterions.[4,5] The theoretical basis for understanding the kinetics of micellar equilibria was provided by Aniansson and Wall[6] (AW) and extensions have been provided by Kahlweit[7] to include the prediction of the observed amplitudes. Excellent agreement is found between the experimental results and theoretical fits.[2,3] The effect of micelle coalescence/fission in nonionic surfactant systems (or at high salt concentrations in ionic systems), originally neglected by AW, has been addressed by Kahlweit.[8]

An estimate of the exit rate kinetics from diblock copolymer micelles based on Kramers[9] rate theory was developed by Halperin and Alexander.[10] They also demonstrated that the AW mechanisms would be dominant for such micelles by calculating the barrier free energies for micelle coalescence and fission. Notably, micelle coalescence is energetically unfavorable owing to steric interactions between the corona chains. Steric hindrance is less pronounced for short chains. Scaling theory, which is valid only for long chains, is employed to calculate the free energy of the micelle, making direct comparison to our results for short chains difficult and at best approximate.

The use of molecular level simulations to investigate the dynamics of self-assembly has been limited owing to the complexity of the problem. Halilo$\tilde{g}$lu and Mattice[11] defined a number of correlation functions to demonstrate that the dynamics for the interchange of chains could be probed in Monte Carlo (MC) simulations. By tagging chains in a specific aggregate they calculated correlation times for chain extraction, chain addition, and chain redistribution in micelles formed by the diblock copolymer $A_{10}B_{10}$. The exit rate was found to be independent of total surfactant concentration while the entry rates were decomposed into contributions from micelle-micelle coalescence and individual monomer insertion. An analogous approach is employed in this work to extract dynamic information. In addition we also probe the effect of temperature on the observed rate and extract information about the size of the energy barrier for chain extraction from a micelle. More importantly, we relate the observed rate constants to those in the AW mechanism and thereby predict the response of the system to perturbations.

Others have used stochastic dynamics (SD) simulations

 0021-9606/98/108(5)/2232/13/$15.00

to investigate the dynamics associated with the gauche-trans dihedral transitions in butane, decane, and heptane.[12,13] The results were compared to theoretical descriptions of rate processes (e.g., transition state theory,[14] Kramers rate theory,[9] and modifications thereof) and to molecular dynamics simulations (MD) of the system including the solvent. The Langevin equation has also been employed along a reaction coordinate in an attempt to determine reaction rates. Recent examples include n-butane isomerization[15] and a particle in a cubic potential.[16] The common feature in past work was that the form of the energy barrier was known, and hence the theoretical approaches could be evaluated by direct comparison to the simulation data. In contrast, no *a priori* knowledge is available about the energy barriers in the micellar system.

The calculation of the frictional coefficient for atoms in polymer chains was addressed by Pastor and Karplus.[17] A methodology based on the accessible surface area exposed by the components of the polymer chain was used to estimate the component's frictional coefficient. The success of this approach was evaluated by comparing the calculated rotational and translational diffusivity to experimental data. Brownian dynamics, in which the inertial terms are neglected, have been employed to determine the bending and twisting dynamics of short linear DNA chains.[18] SD has also been used to investigate dynamic behavior in n-nonane[19] and 1-decanol.[20]

The paper is structured as follows. In Sec. II we describe the simulation algorithm and the model amphiphile that we consider. In Sec. III we begin by briefly reviewing the stepwise association model for surfactant self-assembly. We then determine the exit and entry rate constants associated with surfactant extraction and insertion by monitoring tagged surfactants in the simulations. The Helmholtz free energy associated with the extraction of a surfactant molecule from a micelle is determined by using a thermodynamic perturbation scheme. Subsequently we investigate the response of the system to a perturbation in temperature. Section IV A relates the exit rate constant to the dissociation rate constant, while in Sec. IV B we employ Kramers' rate theory to extract the exit rate constant from the free energy profile. Finally in Sec. IV C we compare our temperature jump results to those predicted using the Aniansson–Wall set of flux equations.

II. SIMULATION DETAILS

The surfactant molecule (A_2B_2) is comprised of a series of particles linked together via rigid, but fully rotatable, bonds. This geometric constraint is imposed iteratively using the SHAKE algorithm.[21,22] The equation of motion for each particle (bead) i within the surfactant is[12]

$$m_i\dot{\mathbf{v}}_i(t) = -m_i\xi_i\mathbf{v}_i(t) + \mathbf{F}_i(\{\mathbf{x}_i(t)\}) + \mathbf{R}_i(t), \tag{1}$$

where m_i is the mass of particle i and $\mathbf{x}_i$, $\mathbf{v}_i$, $\mathbf{F}_i$, and ξ_i represent the position, velocity, force, and frictional (damping) coefficient acting on particle i, respectively. Equation 1 represents the simplest form of stochastic dynamics in which the time and spatial correlations in the frictional coefficient are neglected. The stochastic force $\mathbf{R}_i$ is assumed to be stationary, Markovian and Gaussian with zero mean, and to have no correlation with prior velocities nor with the systematic force. These requirements dictate that $\mathbf{R}_i$ must satisfy the conditions

$$\langle \mathbf{R}_i(t)\rangle = 0, \tag{2}$$

$$\langle R_{i\alpha}(t)R_{j\beta}(t')\rangle = 2k_BT\xi_i m_i\delta_{i,j}\delta_{\alpha,\beta}\delta(t-t'). \tag{3}$$

The indices α, β denote the Cartesian coordinate directions (x,y,z) while i, j denote particle labels. The stochastic noise term acts as a heat bath to compensate for the energy sink due to viscous drag. The stationary solution is the Boltzmann distribution and hence these simulations produce canonical time averages (NVT ensemble).

Unshifted Lennard–Jones (LJ) interactions were employed between the beads, the nature of which could be varied by changing the cut-off distance r_c. The B-B interactions were LJ attractive with a conventional cut-off distance of $r_c = 2.5\sigma$ while A-B and A-A interactions were purely repulsive ($r_c = 2^{1/6}\sigma$). All beads were taken to have equal mass (m) and frictional coefficient (ξ). Bond lengths were constrained to $2^{1/6}\sigma$.

The simulation details and the equilibrium properties at three reduced temperatures form the topic for a previous paper to which the reader is referred.[1] Temperature is expressed in reduced units ($T_r = k_BT/\epsilon$) and a reduced timestep ($t_r = t/\sigma\sqrt{(m/\epsilon)}$) of length $\Delta t_r = 0.005$ was used. ϵ and σ are the well depth and size parameter in the LJ potential. The reduced frictional coefficient is given by $\xi_r = \xi\sigma\sqrt{(m/\epsilon)}$. The total surfactant concentration is defined by $[S] = N_sN_b/V_{sys}$, where N_s is the number of surfactant molecules, N_b is the number of beads per surfactant molecule, and V_{sys} is the simulation volume.

III. MICELLAR DYNAMICS

The exchange of monomers between the bulk solution and micelles may be represented by the reaction

$$A_1 + A_{i-1} \underset{k_i^-}{\overset{k_i^+}{\rightleftharpoons}} A_i, \tag{4}$$

where A_i denotes aggregates with aggregation number i and k_i^+, k_i^- are the association and dissociation rate constants, respectively. The monomer is represented by A_1 in this notation and the concentration of aggregates of size i is $[A_i]$. The rate constants are expected to be a function of the aggregate size i.

It has been demonstrated[1] that the standard state free energy difference, $(\mu_i^o - \mu_1^o)/kT$, is nearly constant for $i > 20$. Therefore $\mu_i^o \approx \mu_{i-1}^o \approx$ constant for $i > 20$. The equilibrium constant may be related to the free energy of formation if the micelles are treated as ideal solutes via

$$K_{eq,i} = \frac{k_i^+}{k_i^-} = \frac{[A_i]}{[A_1][A_{i-1}]} \approx e^{-(\mu_i^o - \mu_1^o)/kT}. \tag{5}$$

The final term is a direct result of the assumed constancy of μ_i^o, i.e., $i\mu_i^o - (i-1)\mu_{i-1}^o - \mu_1^o \approx \mu_i^o - \mu_1^o$. Therefore for

values of $i>20$, the equilibrium constant $K_{eq,i}$ may be considered to be nearly independent of i. Aniansson and Wall,[6] in their theory dealing with kinetics of self-assembly, argued that the improbability of both k_i^- and k_i^+ varying significantly and in a compensating manner to ensure the constancy of $K_{eq,i}$ could be used to infer the relative constancy of k_i^-. This was done in order to solve the flux equations analytically for the short time behavior.

We adopted two approaches to determine the association (k_i^+) and dissociation (k_i^-) rate constants directly from simulation data. The first involved tagging surfactant molecules in aggregates and then monitoring how long it took for them to redistribute among aggregates and the free surfactant pool. The second approach involved calculating the free energy profile for the extraction of a surfactant chain from an aggregate and then using Kramers' rate theory[9] to calculate the exit rate.

A. Exit and redistribution rates

The average exit rate constant was determined by tagging all surfactants in aggregates at $t=0$. The system was then monitored as a function of time. If a surfactant chain left an aggregate (i.e., was no longer within the cut-off distance used to define the aggregate) the chain was detagged. A function $C(t)$ was defined as

$$C(t)=\left\langle \frac{N(t)}{N(0)} \right\rangle, \tag{6}$$

where $N(t)$ is the number of chains still tagged at time t. The angular brackets indicate an average over multiple time origins. Note that all surfactants in aggregates are initially tagged. The contribution of aggregates in the size range $5-20$ is expected to be small, since the number density of these aggregates is very low. Smaller aggregates ($n<5$) may contribute to the short time behavior of $C(t)$ and this will manifest itself as an initial rapid decline in $C(t)$.

The variable $N(t)$ is expected to behave as a first order process, since once a surfactant is detagged it will remain detagged for the remainder of the simulation and therefore a tagged surfactant cannot reenter a micelle

$$\frac{dN(t)}{dt}=-K^-N(t) \tag{7}$$

which yields an exponential form for $C(t)$

$$C(t)=e^{-K^-t}. \tag{8}$$

It is important to note that the exit rate constant defined above, K^-, is related nontrivially to the dissociation rate constant, k_i^-, defined in Eq. (4).

Figure 1 shows the function $C(t)$ at four temperatures at a total surfactant concentration of $[S]=0.12$ and reduced frictional coefficient $\xi_r=0.1$. At the lowest temperature ($T_r=0.50$), the exit rate is slow, so that less than 20% of the initially tagged surfactants have left the micelle phase at a reduced time of $t=500$. The exponential behavior of $C(t)$ is evident at higher temperatures. Small deviations from exponential behavior at short times may be ascribed to the contributions of small labile aggregates that form and breakup easily, as was confirmed by tagging aggregates in a particular size range (e.g., aggregation numbers from 25 to 35) and then calculating $C(t)$. The long time tails of $\ln C(t)$ calculated on the aggregate subset $\{i\}=\{25,35\}$ were found to be parallel to those calculated on the entire aggregate interval $\{2,\infty\}$.

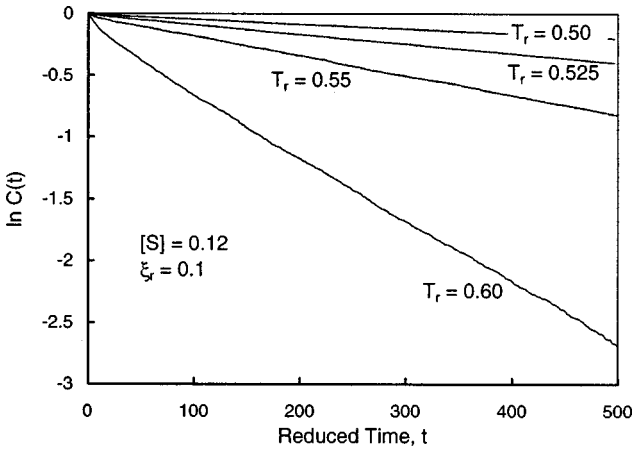

FIG. 1. Effect of temperature on the rate at which tagged chains leave the micelle phase.

The exit rate constant K^- was extracted at each temperature and found to obey an Arrhenius expression

$$K^-=K_o^-e^{-E^*/kT} \tag{9}$$

with an activation barrier energy of E^*, as shown by the linear plots in Fig. 2. The observation that E^* is independent of temperature suggests that the activation energy is far larger than the thermal energy (i.e., a high barrier) and that the micelle structure does not change significantly with temperature. The fact that the free energy difference $(\mu_i^o-\mu_1^o)$ is order 5 kT, is only weakly temperature dependent and nearly constant for $i>20$ is consistent with this requirement.[1] From the slope and intercept in Fig. 2, we obtained $E^*=7.6$ (nondimensionalized by ϵ, the well depth in the LJ potential) and

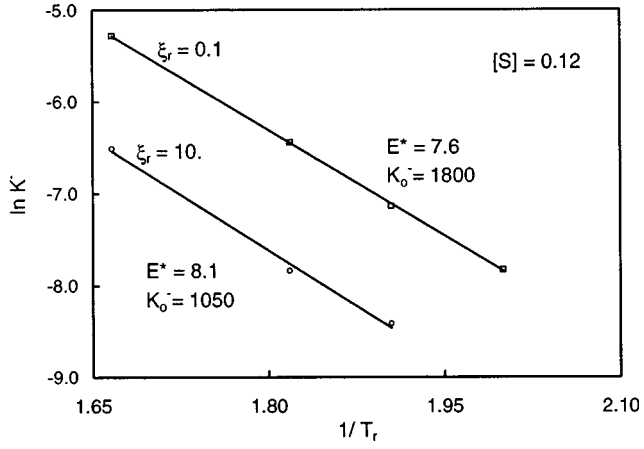

FIG. 2. Arrhenius plot of the exit rate constant K^-. The activation energy, E^*, is found to be independent of ξ_r as expected.

TABLE I. Exit rate constants, K^-, as a function of the frictional coefficient, ξ_r, at $T_r=0.55$ and [S]=0.12.

ξ_r	K^-
0.1	0.0016
0.5	0.0013
1	0.0012
10	0.0004
50	0.0001

$K_o^-=1800$ for $\xi_r=0.1$. The activation energy should be independent of the choice of ξ_r. Figure 2 includes an Arrhenius plot for $\xi_r=10$, for which the activation energy is 8.1 (6% deviation from result at $\xi_r=0.1$). The preexponential term does depend on ξ_r. As ξ_r increases, the surfactant mobility decreases with a concomitant reduction in the preexponential factor K_o^-. The effect of varying the frictional coefficient (at $T_r=0.55$) on the exit rate constant K^- is shown in Table I. As the frictional coefficient increases there is a corresponding decrease in the exit rate constant which may be ascribed to a reduction in surfactant mobility. The functional dependence of the exit rate constant on ξ_r will be discussed in Sec. IV B.

The dynamics associated with the redistribution of surfactants among aggregates may also be used to extract exit and entry rate constants. Towards this end, all surfactants in aggregates are permanently tagged at $t=0$. The number of tagged surfactants that still reside in aggregates, $N(t)$, is then monitored as a function of time and is expected to obey the rate equation

$$\frac{dN(t)}{dt}=-K^-N(t)+K^+[N(0)-N(t)]. \tag{10}$$

As before, we assume that the rate constants are nearly independent of the aggregate size i or alternatively we are content to obtain an average value of the rate constant. The second term on the right of Eq. (10) reflects the fact that tagged surfactants can reenter micelles. Clearly the rate constant K^+ must include the number density of aggregates. The solution of Eq. (10) yields

$$R(t)=\left\langle\frac{N(t)}{N(0)}\right\rangle=\frac{1+\beta e^{-\alpha t}}{1+\beta}, \tag{11}$$

where $\beta=K^-/K^+$ and $\alpha=K^++K^-$. Figure 3 shows a typical two parameter fit (α,β) to the redistribution curve from which the rate constants in Table II were determined. Excellent agreement is obtained between the exit rate constants K^- obtained from these two tagging techniques and this provides some confidence in the K^+ values. However, as is evident in Fig. 3 at long times, definite correlations in the data are evident which are related to correlations in the size distribution during the course of the simulation.

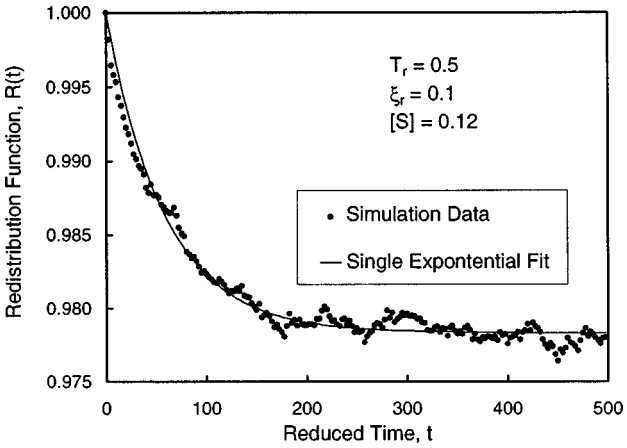

FIG. 3. Redistribution of tagged surfactants among aggregates showing two parameter fit of Eq. (11).

B. Free energy of chain extraction

An alternative approach to calculate the exit/entry rate of a surfactant into a micelle is to determine the free energy profile associated with the process. Rate theory can then be employed to obtain a rate constant.[14]

The free energy profile associated with the extraction of a surfactant chain from a micelle was determined. A typical micelle, aggregation number 38, was taken from an equilibrated system ($T_r=0.50$, [S]=0.12) and used as an initial configuration for small scale SD simulations, with the chosen micelle as the sole aggregate but at the same total surfactant concentration. The micelle was in dynamic equilibrium and was observed to lose and gain monomers throughout the simulation, maintaining an average aggregation number of 37.

A surfactant chain associated with the micelle was chosen at random and the first hydrophobic bead was constrained to lie a distance λ_i from the center of mass of the micelle using the SHAKE algorithm.[21,22] The free energy difference (ΔA_i) associated with a perturbation $\Delta\lambda$ was then calculated via the perturbation relation derived by Zwanzig[23] for a canonical ensemble

$$\Delta A_i=-\mathrm{kT}\,\ln\langle e^{-\Delta U_i/\mathrm{kT}}\rangle_{\lambda_i}. \tag{12}$$

The angular brackets denote an ensemble average over the unperturbed system, but with the constraint λ_i imposed. ΔU_i is the potential energy difference between the perturbed state $U(\lambda_i+\Delta\lambda)$ and its unperturbed value $U(\lambda_i)$. By repeating

TABLE II. Rate constants as a function of reduced temperature, T_r, for $\xi_r=0.1$ and [S]=0.12.

	Exit kinetics, $C(t)$	Redistribution kinetics, $R(t)$	
T_r	K^-	K^-	K^+
0.500	0.0004	0.0004	0.0184
0.525	0.0008	0.0008	0.0213
0.550	0.0016	0.0016	0.0295
0.600	0.0051	0.0055	0.0487

the calculation over a range of λ_i values, a free energy profile may be obtained. This free energy perturbation technique has previously been employed to determine the potential of mean force associated with two solute molecules in a solvent.[24,25] At each value of λ_i we implement two perturbations $\pm\Delta\lambda$, and therefore from N distinct values of λ_i we get $2N$ free energy differences. The value $\Delta\lambda$ is chosen so that $\lambda_{i+1}+\Delta\lambda$ coincides with $\lambda_i-\Delta\lambda$. Therefore by starting at the furthest separation distance (λ_0) and moving towards the center of the micelle, the free energy difference (with respect to a free surfactant chain) at a distance $r_k=\lambda_0-k*\Delta\lambda$ from the micelle center is

$$\Delta A(r_k)=\sum_{j=0}^{k}\overline{\Delta A_j}, \tag{13}$$

where the overbar signifies an average value. An error estimate is obtained for each $\overline{\Delta A_i}$ by subdividing the simulation data into five blocks (n) and determining ΔA_i for each block. The average $\overline{\Delta A_i}$ and standard deviation (σ_i) are therefore accessible,[26]

$$\sigma_i^2(\overline{\Delta A_i})=\frac{\Sigma_{j=1}^{n}(\Delta A_i(j)-\overline{\Delta A_i})^2}{n(n-1)}, \tag{14}$$

where $\Delta A_i(j)$ is the estimate of ΔA_i taken from the jth simulation block. Since $\Delta A(r_k)$ results from a summation over $\overline{\Delta A_i}$'s, the error propagates as we approach the center of the micelle. If the errors may be regarded as independent, the standard deviation at a particular value of k is $\sigma_k=\sqrt{(\Sigma_{i=1}^{k}\sigma_i^2)}$. An alternative procedure would be to calculate an average standard deviation and then an error estimate in $\Delta A(r_k)$ is $\sigma^2(\Delta A(r_k))=k\sigma_{avg}^2$. The free energy profile at $T_r=0.50$ is shown in Fig. 4(a) and a radial distribution profile through the unconstrained micelle is shown in Fig. 4(b).

The implementation of the constraint λ_i may affect the shape of the micelle and the micelle structure. This was not found to be the case for reasonable values of λ_i as inferred from the invariance of the radial distribution profile through the micelle and of the micelle aggregation number with different values of the constraint λ_i. If micelle deformation does occur, the calculated free energy difference will not be representative of chain extraction.

The free energy profile for the extraction of a chain from a micelle of size 29 at $T_r=0.55$ is shown in Fig. 5. At the higher temperature, the micelle is far more labile and the micelle center of mass is constantly changing due to the loss and gain of monomers. This poses a particular problem in trying to constrain a surfactant to be a prescribed distance from the micelle center of mass, especially when, for example, a dimer leaves the micelle. If the imposed constraint failed to converge, a repeat run was performed and the results averaged. Typically six runs were performed per datum point from which an error estimate could be made. Two distinct differences are evident by comparing the free energy profile in Fig. 5 to that for a micelle of size 37 at $T_r=0.50$ shown in Fig. 4(a); (1) the free energy at large radial distances drops off more rapidly for the smaller micelle and (2)

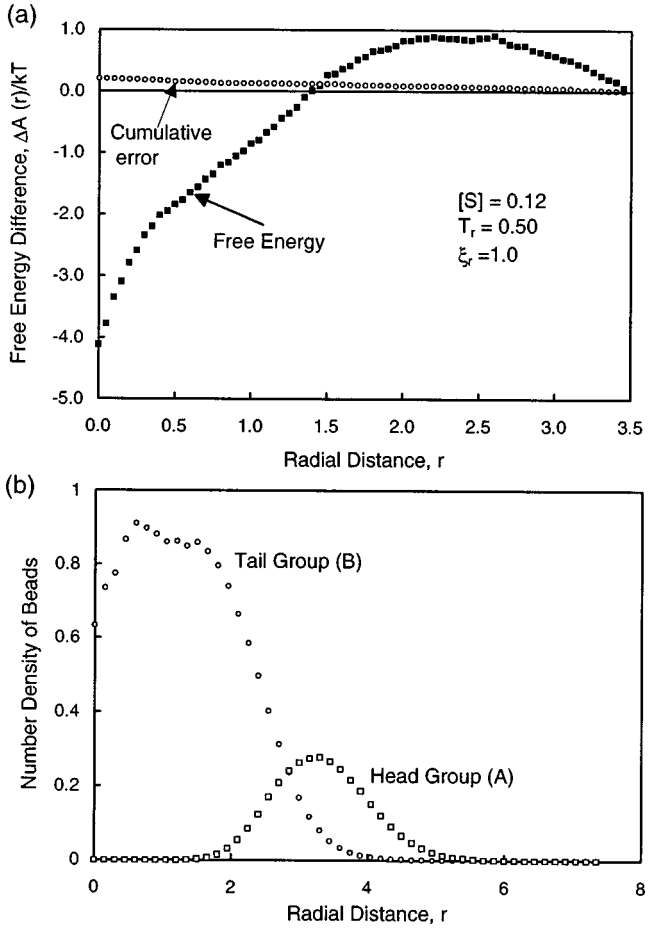

FIG. 4. (a) Free energy profile through micelle of size 37 and cumulative error, as represented by the standard deviation, for each value of the radial distance r. (b) Radial distribution profile through micelle of size 37.

the minimum in the free energy profile is almost 1 kT higher for the smaller micelle at the higher temperature. We have already commented on the constancy of the standard state free energy difference, $(\mu_i^o-\mu_1^o)/kT$, for micelles with $i>20$ and therefore we would not expect the micelle size to affect the barrier height significantly. We therefore conclude

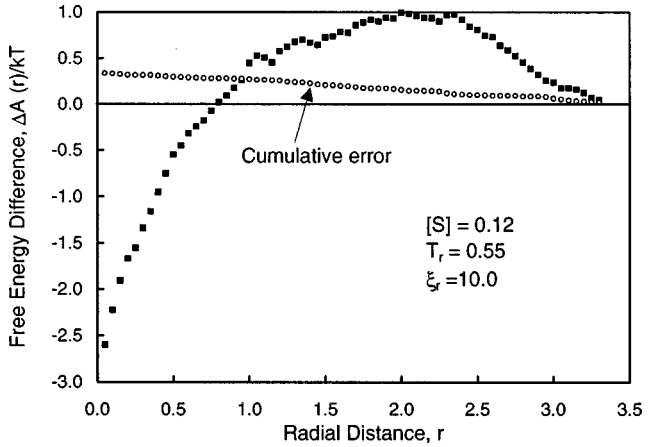

FIG. 5. Free energy profile through a micelle of size 29 at $T_r=0.55$. The cumulative error, as represented by the standard deviation, is shown for each value of the separation distance r.

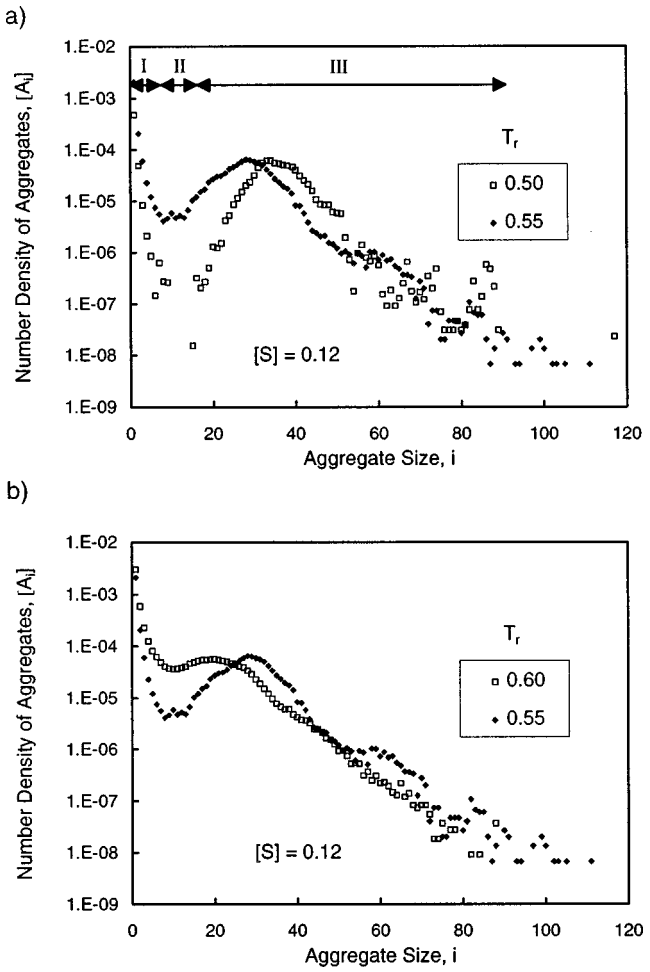

FIG. 6. Size distribution of aggregates at the initial and final temperatures used in the temperature jump simulations. (a) $T_r=0.55$ and $T_r=0.50$ and (b) $T_r=0.55$ and $T_r=0.60$.

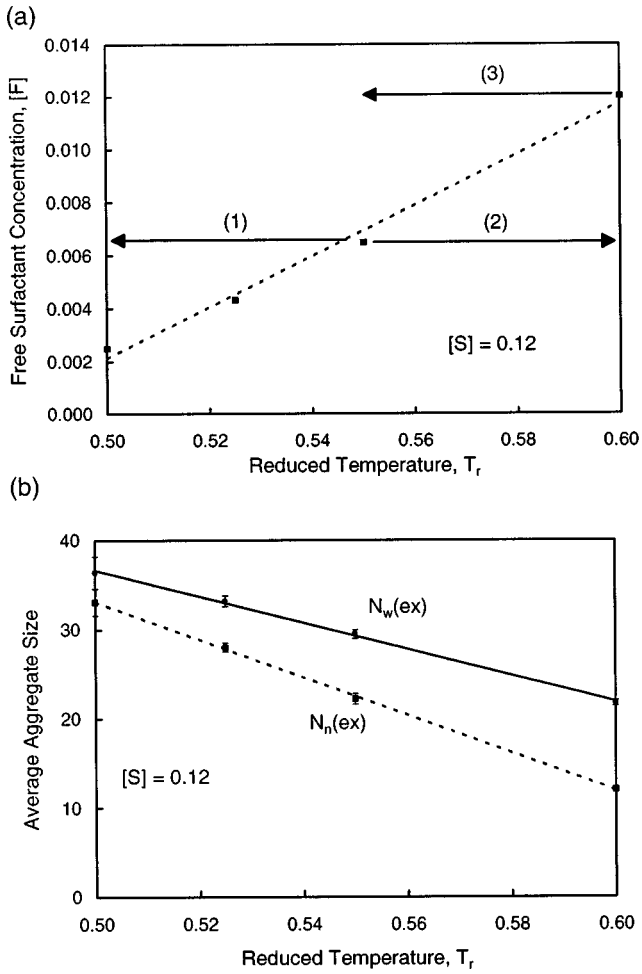

FIG. 7. Equilibrium properties as a function of temperature at [S]=0.12. (a) Free surfactant concentration [F]. The arrows depict the direction and magnitude of the temperature jump ''experiments.'' (b) Number (N_n) and weight averaged (N_w) aggregation number. Error bars indicate ± one standard deviation and are largest at the lowest temperature, $T_r=0.50$, amounting to ± 5%.

that the observed variation in barrier height [compare Fig. 4(a) and Fig. 5] is predominantly due to the difference in temperature.

C. Temperature jump

Temperature jump computer ''experiments'' were performed to elucidate the dynamics involved in forming micelles. An initially equilibrated configuration was subjected to a rapid temperature change to a final temperature, and the response of the system was monitored as a function of time. In order to remove the effect of fluctuations in the instantaneous values, the results were averaged over a number of independent starting configurations. Typically 10–30 runs were required to produce reasonable statistics.

According to the Aniansson–Wall (AW) theory, the presence of two well separated time constants is consistent with a number density of aggregates which fall into three regions as depicted in Fig. 6(a). Region I contains monomers and small aggregates (dimers, trimers, etc.). Region III contains a distribution of micelles (assumed Gaussian by AW). The regions I and III are separated by a depleted zone (region II) where very few micelles are present. The fast process (monomer insertion/removal) is associated with reactions involving the species in Secs. I and III, while the slow process (micelle formation/dissolution) is governed by the low concentration of premicelles within the region II.

A starting configuration at $T_r=0.55$ displaying these three distinct regions was perturbed to a temperature $T_r=0.50$ [i.e., process (1) as depicted in Fig. 7(a)]. The equilibrium properties corresponding to the starting and end points of the temperature jump have been calculated and are presented in Fig. 7. The free surfactant concentration, [F], decreases with decreasing temperature. A decrease in temperature favors the formation of larger aggregates as reflected in the increased number and weight average aggregation numbers (excluding monomers), N_n(ex) and N_w(ex) in Fig. 7(b). These results are consistent with an enthalpically driven micellization process.

The system size was 864 surfactants at a total surfactant concentration of [S]=0.12. The system was initially quenched to its new temperature by performing a short run (duration $t=2.5$) at high frictional coefficient. A production

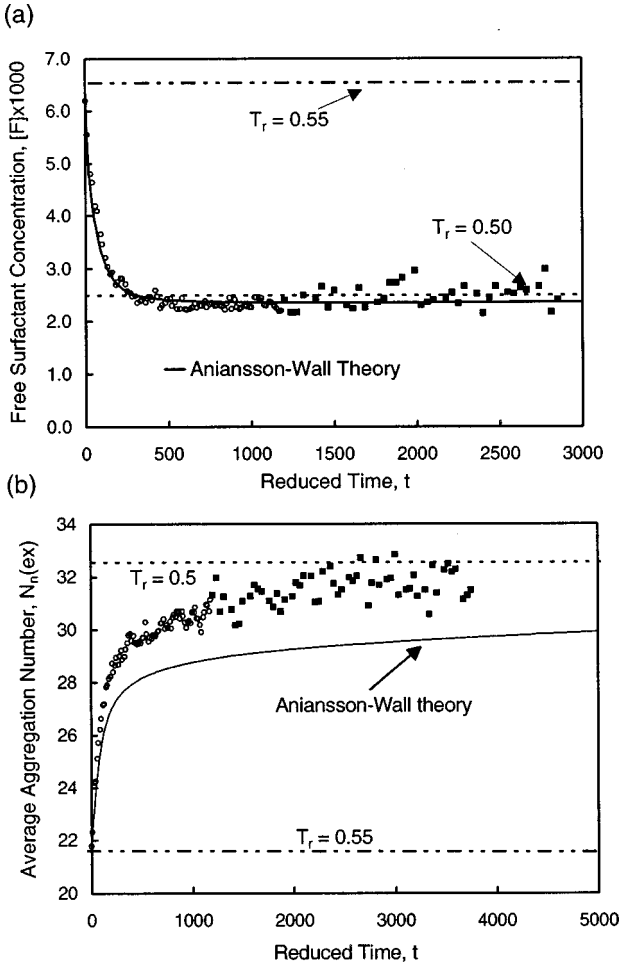

FIG. 8. Comparison of simulated temperature jump data to those predicted using the Aniansson–Wall theory. (a) Time evolution of the free surfactant concentration ([F]) (b) and average aggregation number $[N_n(\mathrm{ex})]$. The solid squares and open circles were obtained by averaging over five and 20 independent initial configurations, respectively.

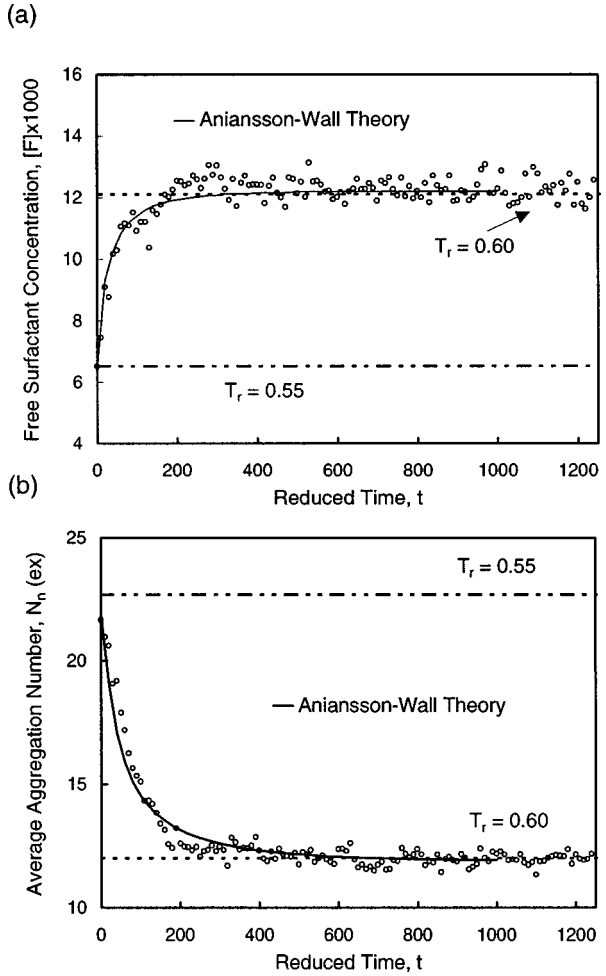

FIG. 9. Temperature jump from $T_r=0.55$ to $T_r=0.60$. (a) Time evolution of the free surfactant concentration ([F]) (b) and average aggregation number $[N_n(\mathrm{ex})]$.

run at $\xi_r=0.1$ was then performed. At low values of the frictional coefficient, the system responds only slowly to the imposed temperature change and the dynamics will be obscured by the dynamics of the temperature jump, therefore the necessity for an initial quenching run. The quenching run ensured a rapid thermal relaxation to the new conditions during which the micellar system remained essentially unchanged. The instantaneous values of the free surfactant concentration, [F], averaged over 20 independent initial configurations, are shown in Fig. 8(a) by the open circles. The system starts at its equilibrium value at $T_r=0.55$ at $t=0$ and decreases rapidly to its final value as indicated by the dashed line. A small overshoot is evident at intermediate times. The free surfactant behavior appears to be well described by a single exponential decay at short times. The evolution of the average aggregate size $[N_n(\mathrm{ex})]$ is shown in Fig. 8(b) and clearly it has not reached its equilibrium value even at $t=1400$. A very slow upward drift is still evident at long times. Five long runs were performed to $t=3800$ to ensure that we did in fact continue to approach the desired final equilibrium state. These data are far more noisy and are differentiated by the solid square markers in Fig. 8. The solid lines in Fig. 8 are theoretical predictions obtained from the Aniansson–Wall equations which will be described in Sec. IV C.

The effect of the friction coefficient was evaluated by repeating the temperature jump at $\xi=0.43$ and $\xi=4.3$, corresponding to a 40-fold variation in the friction coefficient. The results were in qualitative agreement with those obtained at $\xi_r=0.1$, except that far longer runs were required. The long runs made it impractical to average over many initial configurations.

Two further temperature jump runs, as depicted by the direction of the arrows labeled (2) and (3) in Fig. 7, were performed. The corresponding size distributions are shown in Fig. 6(b). Run (2) comprised a temperature increase from $T_r=0.55$ to $T_r=0.60$ and run (3) the equivalent temperature decrease, i.e., the reverse of run (2). These results appear in Figs. 9 and 10 and are discussed in Sec. IV C where we compare the simulation results to the results predicted using the Aniansson–Wall series of flux equations.

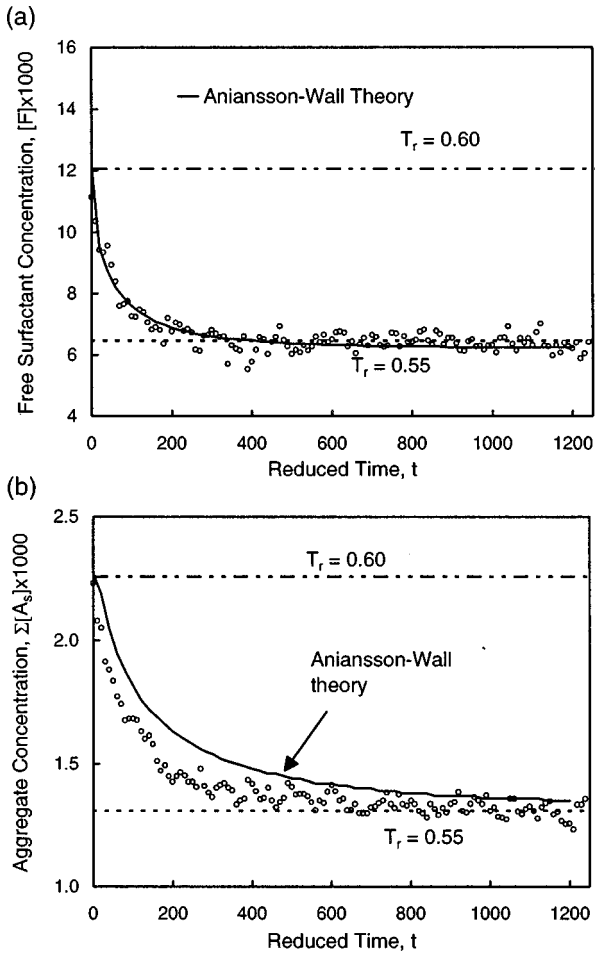

FIG. 10. Temperature jump from $T_r=0.60$ to $T_r=0.55$. (a) Time evolution of the free surfactant concentration ([F]) (b) and aggregate concentration, $\Sigma_{i=2}^{\infty}A_i$.

IV. DISCUSSION

A. Tagging runs

For a simple double well potential, Zhou[27] has shown that for barrier heights greater than 3 kT, the dynamics of barrier crossings can be described by a chemical rate equation. The associated decay in the correlation function is exponential for all values of the friction coefficient. This is confirmed in our work, where the barrier height (order 10–15 kT) is sufficiently large that $C(t)$ is always exponential in form.

The rate constants extracted from exit and redistribution of tagged surfactants, K^- and K^+, need to be related to those of micelle association and dissociation introduced in Eq. (4). This is achieved by considering aggregates of size i that contain j tagged surfactants, which are represented as $A_{i,j}$. The following reactions are possible:

$$A_{1,0}+A_{i,j} \underset{k_{i+1}^-}{\overset{k_{i+1}^+}{\rightleftharpoons}} A_{i+1,j}, \tag{15}$$

$$A_{1,1}+A_{i-1,j-1} \overset{k_i^-}{\leftarrow} A_{i,j}, \tag{16}$$

$$A_{1,0}+A_{i-1,j} \underset{k_i^-}{\overset{k_i^+}{\rightleftharpoons}} A_{i,j}, \tag{17}$$

$$A_{1,1}+A_{i,j} \overset{k_{i+1}^-}{\leftarrow} A_{i+1,j+1}. \tag{18}$$

Equations (15) and (17) are equivalent except for a shift in index i, similarly Eqs. (16) and (18) have both the indices shifted. Equations (16) and (18) represent the expulsion of tagged surfactants which cannot reenter the micelles and correspond to the first set of tagging runs where the tagged surfactants were detagged once they had left the aggregates. The expelled tagged surfactants $A_{1,1}$ are detagged immediately to form $A_{1,0}$, which may in turn reenter micelles. The rate of accumulation of $[A_{i,j}]$ can then be expressed as:

$$\begin{aligned}\frac{d[A_{i,j}]}{dt}=&\left(1-\frac{j}{i+1}\right)k_{i+1}^-[A_{i+1,j}]-k_{i+1}^+[A_{1,0}][A_{i,j}]\\&-\left(\frac{j}{i}\right)k_i^-[A_{i,j}]+k_i^+[A_{1,0}][A_{i-1,j}]-\left(1-\frac{j}{i}\right)\\&\times k_i^-[A_{i,j}]+\left(\frac{j+1}{i+1}\right)k_{i+1}^-[A_{i+1,j+1}].\end{aligned} \tag{19}$$

The number concentration of tagged surfactants which are in aggregates at time t, $N(t)$, is then simply given by

$$N(t)=\sum_{i=2}^{\infty}\sum_{j=0}^{i} j[A_{i,j}] \tag{20}$$

and can be shown using Eq. (19) to evolve via

$$\frac{dN}{dt}=-\frac{k_2^-}{2}N_2-\sum_{i=2}^{\infty}\frac{k_i^-}{i}N_i, \tag{21}$$

where N_i is the concentration of tagged surfactants in aggregates of size i, i.e., $N_i=\Sigma_{j=0}^{i}j[A_{i,j}]$. The additional term involving N_2 reflects the fact that, when a dimer breaks up two free surfactants result, i.e., we lose *two* tagged surfactants. If the additional N_2 contribution is neglected, a comparison of Eq. (7) to Eq. (21) yields the following relationship

$$K^-N(t)\equiv K^-\sum_{i=2}^{\infty}N_i=\sum_{i=2}^{\infty}\frac{k_i^-}{i}N_i. \tag{22}$$

The simulation results suggest that K^- is independent of i and time invariant; and that Eq. (7) is a satisfactory description of the process. Therefore in order for the two descriptions of $N(t)$ to be consistent we must conclude that $K^-=k_i^-/i$. This result is in agreement with our findings that the barrier energy associated with the expulsion of a chain is far larger than the thermal energy, i.e., there is a large energy barrier to this process. Therefore the individual surfactants in a micelle all have equivalent energy in comparison to the barrier height and the probability of a micelle of size i losing a surfactant is given by $i\times$ {the probability of a single chain being expelled}, i.e., the dissociation rate $k_i^-=iK^-$. This result comes as no surprise since the free energy difference for

aggregates with $i>20$ is constant so that one would expect that the barrier height for chain extraction would also be size independent in the micelle region.[1] The result is in agreement with the expression derived by Aniansson *et al.*[3] from the Smoluchowski equation for the dissociation constant

$$k_i^- = i\frac{D_m}{l_b l_o}e^{-\epsilon^*/kT}, \tag{23}$$

where ϵ^* is the activation energy, D_m is the diffusion constant over the barrier, and l_b, l_o are related to the width of the barrier at one kT below its maximum. Obviously these arguments hold only for well defined micelles and cannot be extended into the premicelle region.

The redistribution runs can similarly be described by a set of reactions in which tagged surfactants are allowed to reenter micelles, in which case reactions 16 and 18 are reversible. This yields the following expression for the time evolution of $N(t)$

$$\begin{aligned}\frac{dN}{dt} &= -\frac{k_2^-}{2}N_2 - \sum_{i=2}^{\infty}\frac{k_i^-}{i}N_i + (N(0)-N) \\ &\quad\times\left(k_2^+(N(0)-N) + \sum_{i=2}^{\infty}k_i^+[A_{i-1}]\right) \\ &\approx -\sum_{i=2}^{\infty}\frac{k_i^-}{i}N_i + (N(0)-N)\sum_{i=2}^{\infty}k_i^+[A_{i-1}].\end{aligned} \tag{24}$$

The two additional terms in comparison to Eq. (21) account for the reentry of tagged surfactants into the micelle phase. The term involving k_2^+ accounts for pairs of tagged surfactants associating to form dimers. The approximation made in the last part of Eq. (24) is justified since most surfactants are in the micelle phase and hence the terms involving the summations over the micelles will dominate the observed redistribution kinetics. Once again, by comparison to Eq. (10) we may infer

$$K^+ = \sum_{i=1}^{\infty}k_{i+1}^+[A_i]. \tag{25}$$

In the simulation, the variation of the concentration of aggregates, $[A_i]$, will therefore affect the entry rate constant K^+. The expression for K^+ may be recast using the definition of $K_{eq,i}$ [Eq. (5)] and the approximation for $k_i^- = iK^-$ to give

$$K^+ \approx K_{eq}K^-\left(\sum_{i=1}^{\infty}i[A_i] + \sum_{i=1}^{\infty}[A_i]\right), \tag{26}$$

where the constancy of K_{eq} in the micellar region, which was discussed earlier, is invoked. Therefore from a knowledge of the equilibrium constant K_{eq} (which may be extracted from the size distribution data as will be discussed in Sec. IV C), an estimate for K^+/K^- may be made. For example at $T_r=0.60$, $K_{eq}\approx 300$ and the surfactant concentration $(\Sigma_1^{\infty} i[A_i])$ is 0.03, yielding an estimate $K^+/K^- = 9.0$ which is consistent with the result 8.8 obtained from the tagging runs shown in Table II.

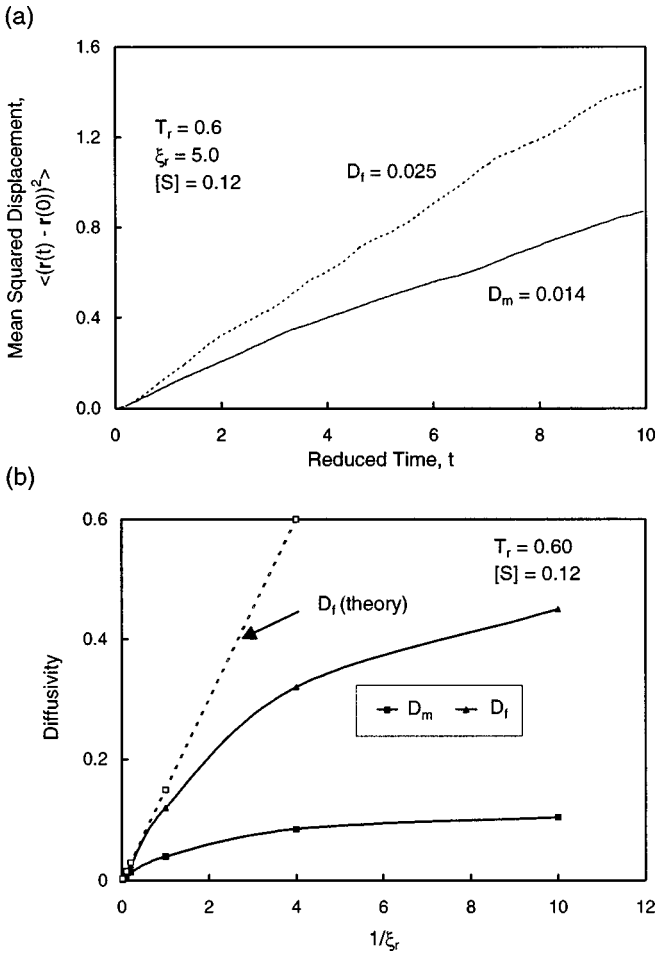

FIG. 11. (a) Mean squared displacement of surfactant center of mass for free and associated surfactants yielding the diffusivity D_f and D_m, respectively from Eq. (27) and (b) effect of the frictional coefficient, ξ_r, on D_f and D_m. The dotted line represent the theoretical result which corresponds to a system at infinite dilution and the open symbols are the corresponding infinite dilution simulation results.

The exit rate constant K^- was found to depend strongly on the frictional coefficient, ξ_r, as shown in Table I. An attempt was made to rationalize these results by relating the observed exit rate to the diffusion coefficient of a surfactant in the micelle phase. The required diffusion coefficients were estimated by calculating the mean squared displacement of the center of mass of the surfactant molecules. Two surfactant diffusivities were calculated, namely that of the unassociated (free) surfactant (D_f) and that of a surfactant in the micelle phase (D_m, neglecting the micelle diffusivity). A representative plot of the mean squared displacement as a function of time is shown in Fig. 11(a). The slope of the linear regression to these plots (at long times) yields the diffusivity via

$$D_\alpha = \frac{\langle|\mathbf{r}_{cm}(t)-\mathbf{r}_{cm}(0)|^2\rangle_\alpha}{6t}, \tag{27}$$

where $\mathbf{r}_{cm}$ represents the center of mass of a surfactant chain and the angular brackets indicate an ensemble average over all surfactant chains in the phase α, either free monomers or

the micelle phase. The diffusivity of the free surfactant, at infinite dilution, should be directly related to the frictional coefficient, ξ_r, since

$$D_f = \frac{T_r}{N_b \xi_r}, \tag{28}$$

where $N_b = 4$ is the number of beads per surfactant chain. This result is confirmed by the calculated infinite dilution diffusivities as shown by the open symbols in Fig. 11(b). The dashed line in Fig. 11(b) corresponds to the theoretical diffusivity at infinite dilution as given by Eq. (28). D_m is an order of magnitude lower than the diffusivity at infinite dilution at small ξ_r and corresponds to the hindered diffusion of the surfactant molecules in the micelle phase due to interactions and collisions with the other surfactant molecules. The measured diffusivity of the free surfactant molecules, D_f, corresponds closely to the theoretically predicted infinite dilution diffusivities at high values of the friction coefficient. However, at small values of ξ_r, the measured diffusivity is one third of that expected at infinite dilution. At large values of the frictional coefficient, the observed diffusivities are determined by the value of ξ_r. At small ξ_r, the motion of the beads is ballistic and the diffusivity is determined by collisions with other molecules and hence provides an indication of the mean free path that the molecule experiences. The measured diffusivity depends on the time scale of observation. If, for example, the root mean squared displacement (rms) of a surfactant molecule in a micelle is calculated, three distinct regions are evident. At short times, the behavior is determined by the frictional coefficient ξ_r. At intermediate times the hindered diffusion within the micelle is important. If we calculate the rms for a sufficiently long period of time, we eventually reach a third linear region, characteristic of micelle diffusion.

B. Chain extraction

The height of the free energy barrier for chain extraction was found to be order of 5 kT for a micelle of size 37 at $T_r = 0.50$ and 3.6 kT for a micelle of size 29 at $T_r = 0.55$. This free energy barrier is sufficiently large compared to the thermal energy that the assumption of a large barrier invoked in the last section is valid. The observed maximum in free energy coincides with the incorporation of the first bead into the hydrophobic domain (Fig. 4).

The activation energy associated with chain extraction, obtained from the Arrhenius plot of the exit rates, was of order 10–15 kT. If it is assumed that the dominant contribution to the activation energy is the removal of the surfactant beads from the interior of a micelle, then the activation energy is readily estimated as the product of the strength of B-B interactions and the number of interactions per surfactant molecule. The former is simply ϵ_{BB}. The latter is, at most, the lattice coordination number per bead, z, times the number of B beads per molecule, n_B. A better estimate recognizes that much of the surrounding volume is occupied by solvent or by A beads, so that the upper bound is multiplied by the average number density of B beads in the core region of the micelle, ρ_B. Thus the following approximation for the activation energy may be made,

$$\Delta U = (\rho_B z n_B)\epsilon_{BB} = (0.5 \times 11 \times 2)(-1) = -11 \approx -20 \text{ kT}. \tag{29}$$

Note that the A-B and A-A interactions do not contribute since these interactions are purely LJ repulsive ($\epsilon_{AB} = \epsilon_{AA} = 0$). The estimate of $\rho_B = 0.5$ is based on the radial distribution profile obtained for a micelle of size 30 as presented in a previous paper.[1]

In comparison to the activation energy obtained from the Arrhenius plot of the exit rate, the free energy barrier for chain extraction is roughly 50% lower than the Arrhenius energy barrier for the exit kinetics. The difference may be ascribed to the negative entropic contribution of packing chains within the micelle.

The association rate constant (k_i^+) is expected to be diffusion controlled, due to the small free energy barrier associated with insertion of a monomer into a micelle (order 1 kT). This is in agreement with the results of Aniansson *et al.*[3]

Since the relevant driving force in our system is the Helmholtz free energy, we are now in a position to determine the surfactant exit rate using rate theory. In particular, the analytical solution of the probability distribution in phase space (the Fokker–Planck equation) for noninteracting Brownian particles in a potential well has been solved by Kramers[9,28] to yield

$$K^- = \frac{\Omega}{2\pi}\left(\sqrt{\left(\frac{\eta^2}{4\omega^2} + 1 \right)} - \frac{\eta}{2\omega} \right) e^{-F^*/kT}, \tag{30}$$

where Ω and ω represent the frequencies of the well and the peak of the free energy profile (assumed quadratic in form) with barrier of height F^*. η is the effective frictional coefficient of the Brownian particle (in our case the actual diffusion coefficient of the monomer in the micelle). In the limit of low friction, the transition state theory rate constant is recovered. As noted by Kramers,[9] Eq. (30) is inappropriate at small η because it ignores the effects of depopulation below the barrier top. The rate should then be determined by considering the slow diffusion of the Brownian particle along the energy axis.[9,28]

From the free energy profile at $T_r = 0.55$, we obtain $F^*/\text{kT} = 3.6$, $\Omega \approx 3$, and $\omega \approx 0.5$. The values of Ω and ω are clearly approximate since they assume that the energy well and barrier can be described by a quadratic expression in the reaction coordinate. The effective frictional coefficient, η, for a surfactant in a micelle was determined from the measured diffusion coefficients ($\eta = T_r / N_b D_m$) and lies in the range 2–100 depending on ξ_r. In our case, $\eta > \omega$, i.e., we have large to moderate damping within the micelle and Eq. (30) is therefore appropriate. The predicted exit rate as a function of η is shown in Fig. 12 and is in qualitative agreement to the results obtained from tagging runs (Table I). Clearly, comparing the results in Table I to Fig. 12, the shift in the frictional coefficient is consistent with the fact that the

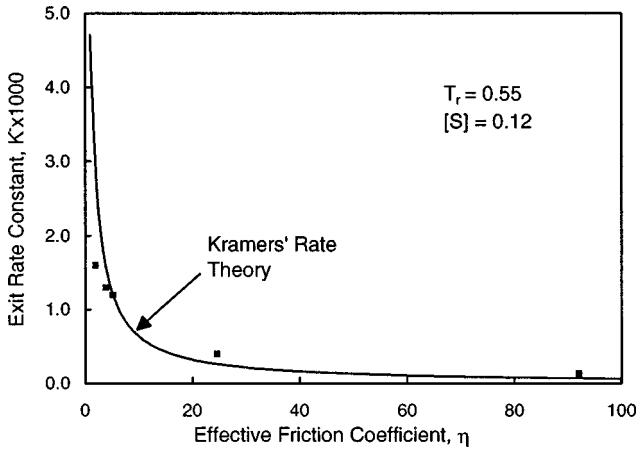

FIG. 12. Variation of the surfactant exit rate (K^-) with friction coefficient (of monomer in micelle) as predicted using Kramers' rate theory and the free energy profile for chain extraction at $T_r=0.55$. Symbols indicate exit rates determined from tagging simulations.

friction coefficient in Fig. 12 corresponds to that of the monomer in the micelle. Therefore the effective frictional coefficient (obtained from the measured surfactant diffusivity in the micelle) was used to plot the simulation data in Table I yielding the square symbols in Fig. 12. The predictions obtained using Kramers' rate theory are in good agreement with the exit rates obtained from tagging runs, except at low values of η.

C. Temperature jump

The ability to calculate the dissociation constant k_i^- in the previous section provides the necessary information to evaluate the predicted response of the system to a perturbation using the flux equations derived by Aniansson and Wall.[6] The deviation from the equilibrium concentration at some instant of time t, $\zeta_i(t)$, is defined as

$$\zeta_i(t)=\frac{[A_i(t)]-[A_i^{eq}]}{[A_i^{eq}]} \tag{31}$$

and evolves via the flux equation

$$[A_i^{eq}]\frac{d\zeta_i}{dt}=J_i-J_{i+1} \quad \text{for } i\geqslant 2, \tag{32}$$

where $J_i=-k_i^-[A_i^{eq}]\{\zeta_i-\zeta_{i-1}-\zeta_1(1+\zeta_{i-1})\}$ is the flux of aggregates to i from $i-1$. Therefore provided that the initial deviation from equilibrium $[\zeta_i(0)]$, the final equilibrium concentration of all species ($[A_i^{eq}]$), and the dissociation rate constant k_i^- are known, the set of equations [Eq. (32)] may be integrated numerically in time. The monomer concentration is obtained from the mass balance constraint. We are therefore in a position to evaluate the proposed mechanism of Aniansson and Wall by direct comparison to the temperature jump experiments described earlier.

In the previous section we evaluated the dissociation rate k_i^- from simulation data. We found that $k_i^-=iK^-$ and concluded that this is a reasonable approximation for i in the micellar region. At low aggregation numbers one would expect the dissociation constant to increase, a reflection of the labile nature of the small premicellar aggregates. In the premicellar region it is reasonable to assume that the association rate is diffusion controlled, i.e., $k_i^+\approx$constant, and hence from a knowledge of the equilibrium constant $K_{eq,i}$, we may extract the dissociation rate constant. The dissociation rate constant and measured equilibrium constant are shown in Figs. 13(a) and 13(b), respectively. At low temperature ($T_r=0.55$ and $T_r=0.50$) the simulated data are noisy, particularly in the depleted zone where very few micelles exist and hence very long runs are required to obtained reasonable statistics. Over the range $i=1\rightarrow 15$ a linear dependence of K_{eq} on i was assumed as shown in Fig. 13(b) (this was necessary only at low temperatures where the statistics in the depleted zone were inadequate). A matching condition at $i=15$ was imposed in order to evaluate the association constant and hence extract the dissociation constant shown in Fig. 13(a).

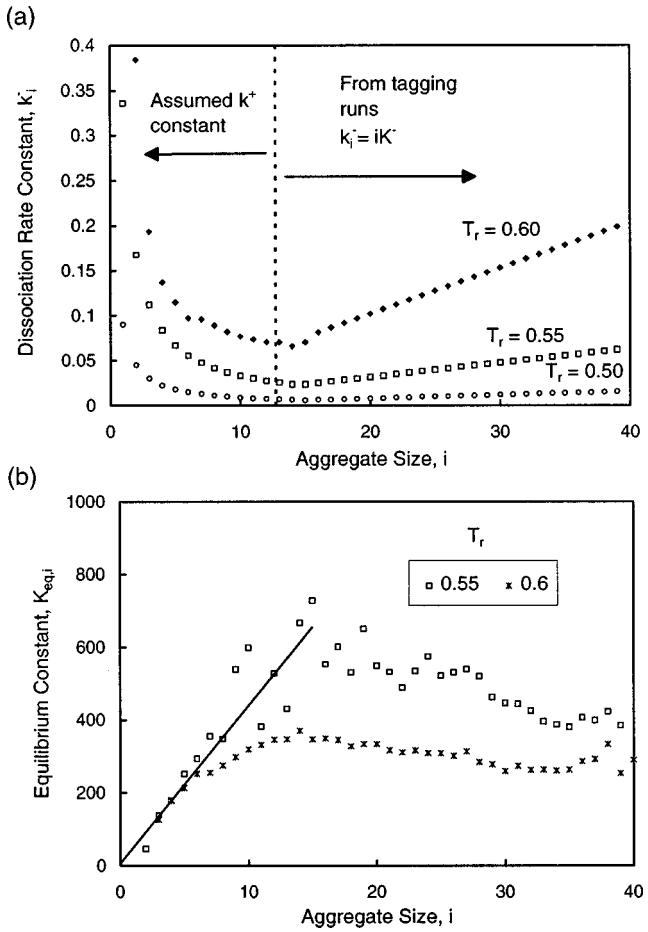

FIG. 13. (a) Estimated dissociation rate constant (k_i^-) used in the solution of the Aniansson–Wall flux equations at [S]=0.12. (b) Equilibrium constant, $K_{eq,i}$, as a function of aggregation number.

For $T_r=0.50$, size distribution simulation data were fit using a Gaussian function in the micelle region (region III) and a single exponential in region I (oligomers). A fitted function was required for the AW theory, to smooth the statistical error associated with the simulation data in the depleted zone (region II).

A comparison between the simulated temperature jump

results and those obtained from the Aniansson–Wall theory is shown in Fig. 8. The time evolution of the free surfactant concentration is found to be in excellent agreement. In fact, the Aniansson Wall theory suggests that the free surfactant concentration dips below its final equilibrium value returning to its equilibrium value only after $t=50\,000$. A similar result was found from the simulation data [Fig. 8(a)] except that the time scale associated with the second process was far more rapid in the simulations. This is clearly shown in the transient behavior of the average aggregation number N_n (ex) (definition excludes monomers) shown in Fig. 8(b). The agreement between AW theory and the simulated data is good at short times but deviates considerably after $t=1000$. The AW theory predicts a far slower second relaxation process (tenfold slower).

Two further temperature jump computer experiments were performed as depicted by the arrows (2) and (3) in Fig. 7. Run (2) monitored the response of the system to an increase in temperature and therefore enabled us to probe micelle dissolution. The results are shown in Fig. 9. The Aniansson–Wall theory was used, as described previously, to predict the system response. Similar results are shown in Fig. 10 for the quench from $T_r=0.60$ to $T_r=0.55$. A significant concentration of aggregates is present in the micelle depleted zone [Fig. 6(b)] and therefore it was unnecessary to fit a functional form to the data as was done in the analysis of run (1). Also, at the higher temperatures, the equilibrium statistics are better as shown by the calculated $K_{eq,i}$ values given in Fig. 13(b) at $T_r=0.60$. Excellent agreement is obtained in predicting the response of the system to an increase in temperature. The micelles expel monomers and the average aggregation number, N_n(ex), decreases. On forming micelles [run (3)] the agreement is not as good. The free surfactant concentration is well described, but the Aniansson–Wall formalism predicts a slower response in the number concentration of aggregates and N_n(ex). As the depth and width of the depleted zone decrease so does the difference between the first and second relaxation times. The results for the temperature jump runs (2) and (3) are asymmetric since the response of the system is determined by the size distribution at the final equilibrium temperature (Fig. 6).

In summary, the first, fast process, associated with monomer insertion, is well described by the AW theory and suggests that the independently extracted rate constants for $i>20$ are in fact correct. The second, slow process, associated with the formation and dissolution of micelles, is not well described. The slow process is determined by the concentration and rate constants in the depleted zone (region II). Micelle—micelle coalescence, which is not accounted for in the AW theory, is observed in the simulation and may account for some of the observed deviation. However, the approximations made in determining the rate constants for $i<20$ are believed to be the dominant reason for any discrepancy.

V. CONCLUSION

Information about the dynamics involved in micellar systems was extracted using stochastic dynamic simulations and interpreted based on the available theory of Aniansson and Wall. In particular, by tagging surfactants in micelles, we have been able to evaluate a surfactant exit rate constant and relate this to the dissociation rate constant used in the stepwise association model of surfactant self-assembly. An activation energy of approximately 10–15 kT for chain extraction was obtained from the temperature dependence of the exit rate constant. A Helmholtz free energy profile for chain extraction was also evaluated. The free energy barrier for monomer insertion was order 1 kT and therefore the association rate is diffusion controlled. The free energy barrier to surfactant removal was of the order 5 kT.

The dissociation rate constants, together with the equilibrium number density distributions were used to evaluate numerically the Aniansson–Wall set of flux equations that describe the response of a system to a perturbation. The AW predicted response of the system to a temperature perturbation was compared to temperature jump computer ''experiments.'' Excellent agreement was obtained for the short time behavior which is associated with monomer insertion. Large deviations in the long time behavior, associated with the growth and dissolution of micelles, were ascribed to errors in estimating the dissociation rate and number density of aggregates in the all important micelle depleted zone. Far better agreement was obtained between AW predictions and simulated results at higher temperatures where the sampling statistics were better, due to a reduction in the depth of the depleted zone.

ACKNOWLEDGMENTS

This work was supported by the National Science Foundation (CTS-9210737) and NASA (NAG 8-951).

[1] F. K. von Gottberg, K. A. Smith, and T. A. Hatton, J. Chem. Phys. **106**, 9850 (1997).
[2] J. Lang, C. Tondre, R. Zana, R. Bauer, H. Hoffman, and W. Ulbricht, J. Phys. Chem. **79**, 276 (1975).
[3] E. A. Aniansson, S. N. Wall, M. Almgren, H. Hoffmann, I. Kielmann, W. Ulbricht, R. Zana, J. Lang, and C. Tondre, J. Phys. Chem. **80**, 905 (1976).
[4] R. J. Hunter, *Foundations of Colloid and Interface Science Vol. 1* (Clarendon, Oxford, 1991).
[5] H. Wennerström and B. Lindman, Phys. Rep. **52**, 1 (1979).
[6] E. A. G. Aniansson and S. N. Wall, J. Phys. Chem. **78**, 1024 (1974).
[7] M. Kahlweit and M. Teubwer, Adv. Colloid Interface Sci. **13**, 1 (1980).
[8] M. Kahlweit, Pure Appl. Chem. **53**, 2069 (1981).
[9] H. A. Kramers, Physica (Amsterdam) **7**, 284 (1940).
[10] A. Halperin and S. Alexander, Macromolecules **22**, 2403 (1989).
[11] T. Haliloğlu and W. L. Mattice, Chem. Eng. Sci. **49**, 2851 (1994).
[12] W. F. van Gunsteren, H. J. C. Berendsen, and J. A. C. Rullmann, Mol. Phys. **44**, 69 (1981).
[13] R. M. Levy, M. Karplus, and J. A. McCammon, Chem. Phys. Lett. **65**, 4 (1979).
[14] S. Glasstone, K. J. Laidler, and H. Eyring, *The Theory of Rate Processes* (McGraw-Hill, New York, 1941).
[15] S. Z. Wan, Y. W. Xu, and C. X. Wang, J. Chem. Phys. **102**, 4976 (1995).
[16] R. Rey, J. Chem. Phys. **104**, 1966 (1996).
[17] R. W. Pastor and M. Karplus, J. Phys. Chem. **92**, 2636 (1988).
[18] S. Allison, R. Austin, and M. Hogan, J. Chem. Phys. **90**, 3843 (1989).
[19] T. Xiang, F. Liu, and D. M. Grant, J. Chem. Phys. **95**, 7576 (1991).
[20] F. Liu, W. J. Horton, C. L. Mayne, T. Xiang, and D. M. Grant, J. Am. Chem. Soc. **114**, 5281 (1992).
[21] J.-P. Ryckaert, G. Ciccotti, and H. J. C. Berendsen, J. Comput. Phys. **23**, 327 (1977).

[22] W. F. van Gunsteren and H. J. C. Berendsen, in *NATO Advance Science Institute Series, The Physics of Superionic Conductors and Electrode Materials*, edited by J. W. Perram (Plenum, New York, 1980), p. 221.
[23] R. W. Zwanzig, J. Chem. Phys. **22**, 1420 (1954).
[24] P. Linse, J. Am. Chem. Soc. **115**, 8793 (1993).
[25] M. Pellegrini and S. Doniach, J. Chem. Phys. **103**, 2696 (1955).
[26] J. M. Haile, *Molecular Dynamics Simulations: Elementary Methods* (Wiley, New York, 1992).
[27] H-X. Zhou, Chem. Phys. Lett. **164**, 285 (1989).
[28] V. I. Mel'nikov and S. V. Meshkov, J. Chem. Phys. **85**, 1018 (1986).